BIOCHEMISTRY
including biophysical chemistry & molecular biology

Article

pubs.acs.org/biochemistry

Effect of Locked Nucleic Acid Modifications on the Thermal Stability of Noncanonical DNA Structure

Jhimli Bhattacharyya,[†] Souvik Maiti,*[,‡] Sanjukta Muhuri,[†] Shu-ichi Nakano,[†,§] Daisuke Miyoshi,*[,†,§] and Naoki Sugimoto*[,†,§]

[†]FIBER (Frontier Institute for Biomolecular Engineering Research), Konan University, 7-1-20 Minatojima-minamimachi, Chuo-ku, Kobe 650-0047, Japan

[‡]Institute of Genomics and Integrative Biology, CSIR, Mall Road, Delhi 110 007, India

[§]FIRST (Faculty of Frontiers of Innovative Research in Science and Technology), Konan University, 7-1-20 Minatojima-minamimachi, Chuo-ku, Kobe 650-0047, Japan

Supporting Information

ABSTRACT: We studied the kinetic and thermodynamic effects of locked nucleic acid (LNA) modifications on parallel and antiparallel DNA duplexes. The LNA modifications were introduced at cytosine bases of the pyrimidine strand. Kinetic parameters evaluated from melting and annealing curves showed that the association and dissociation rate constants for the formation of the LNA-modified parallel duplex at 25.0 °C were 3 orders of magnitude larger and 6 orders of magnitude smaller, respectively, than that of the unmodified parallel duplex. The activation energy evaluated from the temperature-dependent rate constants was largely altered by the LNA modifications, suggesting that the LNA modifications affected a prenucleation event in the folding process. Moreover, thermodynamic parameters showed that the extent of stabilization by the LNA modification for parallel duplexes (3.6 kcal mol^{-1} per one modification) was much more significant than that of antiparallel duplexes (1.6 kcal mol^{-1}). This large stabilization was due to the decrease in $\Delta H°$ that was more favorable than the decrease in $T\Delta S°$. These quantitative parameters demonstrated that LNA modification specifically stabilized the noncanonical parallel duplex. On the basis of these observations, we succeeded to stabilize the parallel duplex by LNA modification at the physiological pH. These results can be useful in the rational design of functional molecules such as more effective antisense and antigene strands, more sensitive strands for detection of target DNA and RNA strands, and molecular switches responding to solution pH.

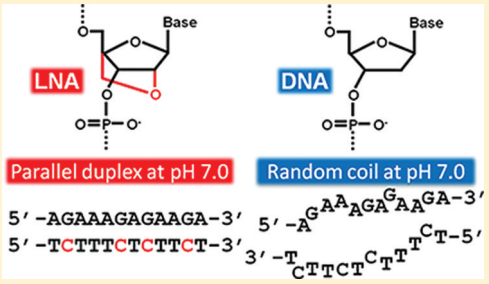

The locked nucleic acid (LNA), containing a methylene linkage between the 2′-oxygen and 4′-carbon in the ribose ring (Scheme 1A), forms a class of modified nucleotides of immense interest.[1−3] Biochemical and biophysical studies have shown that LNA has a high affinity and specificity for the target strand.[4−9] Because of these properties, LNA has been used as probes in DNA sequencing, automated SNP genotyping, capture and detection of various RNAs, gene repair, and particle-mediated delivery of functional peptides.[3] Therefore, an improved understanding of the stabilization mechanism by LNA modification is beneficial for diverse research and industrial applications. To determine the origin of the enhanced stability for LNA modifications, thermodynamics and kinetics of hybridization of LNA-modified oligonucleotides in the canonical duplex structure involving DNA/DNA, DNA/RNA, and RNA/RNA duplexes have been studied.[5,10−16] The effects of LNA on the RNA/2′-*O*-methyl RNA duplex were also reported.[17,18] It has been demonstrated that in general LNA modification enthalpically favors duplex formation because of the more efficient stacking of bases in duplexes resulting in an A-type helical conformation.[5,14,15,18,19] Increments of the number of LNA substitutions led to a favorable entropic change because of the restriction of ribose and the preorganization of the single-stranded state.[5,18,19] Moreover, stabilization by LNA modification is sequence-dependent, including adjacent bases.[19] With respect to the sequence-dependent LNA effects, Bartik used isosequential DNA/DNA and LNA/DNA duplexes and reported that LNA modification in a G-C base pair is more stabilized than that in an A-T base pair.[20] These results allow us to design a thermally and thermodynamically stable duplex of an LNA-containing strand with a target strand.

On the other hand, nucleic acids can fold to form not only the canonical duplex but also the noncanonical structures such as triplex and quadruplex in parallel and antiparallel strand orientations with Hoogsteen base pairs.[21−25] These noncanonical structures play pivotal roles in various biological processes such as regulation of gene expression.[21−25] Thus, controlling the thermodynamics of the noncanonical structures by LNA is currently of interest. In fact, extensive studies have revealed the effects of LNA on the structure and stability of

Received: March 31, 2011
Revised: July 20, 2011
Published: July 21, 2011

Scheme 1. (A) Chemical Structure of LNA, (B) Schematic Illustrations of Structures of PuP/Py0 Depending on pH, and (C) Schematic Illustrations of Structures of PuAP/Py0 Depending on pH

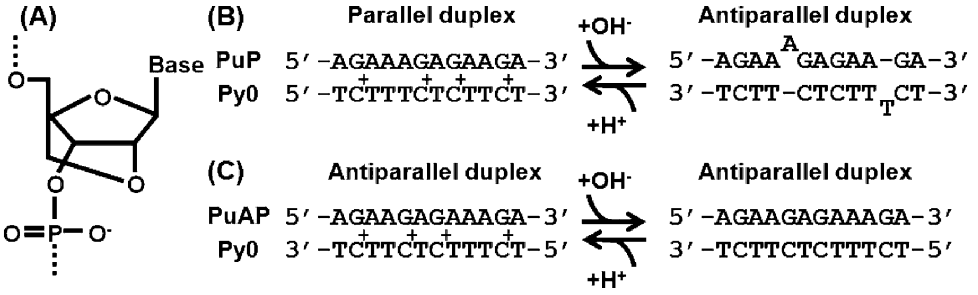

triplex, quadruplex, and further structural competition between Watson–Crick duplex and Hoogsteen quadruplex.[26−34] It has been shown that the stabilization of triplex structure by LNA modification depends on the number and position of LNA modifications, buffer conditions such as pH, and strand orientation (parallel and antiparallel). Although there are rules for designing stable triplex-forming oligonucleotides with LNAs,[28] it is still difficult to generalize how LNA modification affects the thermodynamics of nucleic acid structures. This is partly because the structures and sequences used in these studies were different from each other, making direct comparison quite difficult.

To investigate directly and quantitatively the effects of LNA modification on the canonical antiparallel DNA duplex with Watson–Crick base pairs and the noncanonical parallel duplex with Hoogsteen base pairs, we designed and synthesized antiparallel-stranded and parallel-stranded DNA duplexes with the same nucleotide content composed of Watson–Crick and Hoogsteen base pairs, respectively. Thermodynamic parameters at 25.0 °C evaluated from equilibrium and nonequilibrium thermal melting curves showed that the LNA modification stabilized the parallel duplex by 3.6 kcal mol^{-1} per modification, which is a significantly greater stabilization than that in the antiparallel duplex. This large stabilization was due to the decrease in $\Delta H°$ that is more favorable than the decrease in $T\Delta S°$. The kinetic analysis of the nonequilibrium melting curves further indicated a correlation between the thermodynamic and kinetic parameters for the formation of parallel duplex with the LNA modification. On the basis of these results, we further succeeded in stabilizing the parallel duplex by LNA modifications at physiological pH, which is useful in designing an oligonucleotide hybridizing to a target molecule in a parallel manner.

MATERIALS AND METHODS

Materials and Buffer Preparation. All of the unmodified and LNA-modified oligonucleotides used here were purchased from Hokkaido System Science (Sapporo, Japan) and Gene design Inc. (Ibaragi, Japan), respectively, and were high-performance liquid chromatography (HPLC) grade. The concentrations of the single strands were determined optically by measuring the absorbance at 260 nm at a high temperature using a Shimadzu 1700 spectrophotometer (Shimadzu, Kyoto, Japan) connected to a thermo-programmer. Single-strand extinction coefficients were calculated from mononucleotide and dinucleotide data using the nearest-neighbor approximation.

All the solutions were prepared in Robinson Britton (RB) buffer [35,36] containing 40 mM boric acid, 40 mM phosphoric acid, 40 mM acetic acid, and 100 mM NaCl at various pH values adjusted with 0.2 M NaOH.

Circular Dichroism (CD) Spectroscopy. CD spectra were recorded using a JASCO (Hachioji, Japan) J-820 spectropolarimeter at 4.0 °C in a 0.1 cm path length quartz cell with various concentrations of the oligonucleotides. All spectra were recorded between 200 and 350 nm by taking the average of at least three scans. The sample temperature was maintained with a JASCO PTC-348 temperature controller, and the cell holding chamber was flushed with a constant stream of dry N_2 gas to prevent condensation of water on the external walls of the cell. Before the measurement, the sample was heated to 90.0 °C, gently cooled at a rate of 0.5 °C min^{-1}, and incubated at 4.0 °C overnight.

UV Spectroscopy. The UV absorbance spectra were recorded with a Shimadzu 1700 spectrophotometer equipped with a temperature controller using both 1 and 0.1 cm path-length quartz cuvette. The cuvette holding chamber was flushed with a constant stream of dry N_2 gas during low-temperature measurements to prevent condensation of water on the exterior of the cuvette. The heating and cooling rate was 0.5 °C min^{-1} for all the experiments. Before the measurement, the sample was heated to 90 °C, gently cooled at a rate of 0.5 °C min^{-1}, and incubated at 4.0 °C overnight. Annealing and melting curves were obtained by measuring the UV absorbance at 260 and 295 nm in buffers. The thermodynamic parameters ($\Delta H°$,$\Delta S°$, and $\Delta G°$ at 25.0 °C) were calculated from the melting curves with no hysteresis by fitting with a theoretical equation described previously.[37,38]

Kinetic Analysis. In some cases, the thermodynamic parameters could not be calculated directly from the UV melting curves because of hysteresis. Thus, the thermal curves were analyzed kinetically as follows.[39,40] Using a two-state model, the equilibrium between the single strands and the duplex can be written as

$$\text{DNA single strand (S1)} + \text{DNA–LNA single strand (S2)} \rightleftarrows \text{duplex (D)} \quad (1)$$

The rate of duplex formation is given below, where k_{on} is the rate constant of annealing or cooling (association) and k_{off} is the rate constant of melting or heating (dissociation).

$$d[D]/dt = k_{on}[S1][S2] - k_{off}[D] \quad (2)$$

From the experimental absorbance versus temperature curves, the mole fraction of duplex, α, at each temperature is calculated

dx.doi.org/10.1021/bi200477g | Biochemistry 2011, 50, 7414–7425

from the heating and cooling curves by

$$\alpha = \Delta\mathrm{Abs}/(\mathrm{Abs}_{\min} - \mathrm{Abs}_{\max}) \text{ and}$$

$$\Delta\mathrm{Abs} = [\mathrm{Abs}_{(\text{at any temp})} - \mathrm{Abs}_{\max}]$$

where $\alpha = 1$ for hybridization to form a duplex and $\alpha = 0$ for dissociation of the duplex to single strands. Substituting α in eq 2 gives

$$d(\alpha_h)/dt = k_{on}C(1 - \alpha_h)^2 - k_{off}(\alpha_h) \quad (3a)$$

$$d(\alpha_c)/dt = k_{on}C(1 - \alpha_c)^2 - k_{off}(\alpha_c) \quad (3b)$$

where α_h and α_c are the association factors for heating and cooling curves, respectively, and C is the molar concentration of the single strands (equal stoichometric ratios of the single strands were taken).

Substitution of the heating and cooling rate, dT/dt, in eqs 3a and 3b yields two linear equations with two variables, k_{on} and k_{off}

$$d(\alpha_h)/dT = (dT/dt)^{-1}[k_{on}C(1 - \alpha_h)^2 - k_{off}(\alpha_h)] \quad (4a)$$

$$d(\alpha_c)/dT = -(dT/dt)^{-1}[k_{on}C(1 - \alpha_c)^2 - k_{off}(\alpha_c)] \quad (4b)$$

where $dT/dt = 0.5$ °C/min = 0.00833 K/s.

$k_{on}C$ and k_{off} were determined at different temperatures, T, near the melting temperature of the duplex. In practice, the calculation was conducted at each integer value of T, with $d\alpha/dT$, at a particular temperature T, approximated by $0.5(\alpha_{T+1} - \alpha_{T-1})$. The values of $k_{on}C$ and k_{off} obtained by the method outlined were plotted in Arrhenius plots, $\ln(k_{on}C)$ and $\ln(k_{off})$ versus $1/T$, respectively, giving a positive slope for $k_{on}C$ and a negative slope for k_{off}. Thus, the activation energy, E_{on}, for association is negative and the activation energy, E_{off}, for dissociation is positive.

RESULTS AND DISCUSSION

Sequence Design. The parallel-stranded duplex consisting of PuP (5′-AGAAAGAGAAGA-3′) and Py0 (5′-TCTT-TCTCTTCT-3′) was designed to form fully matched base pairs in the parallel orientation with protonation of cytosines at lower pH, whereas at higher pH, the antiparallel duplex would be formed with two bulges (Scheme 1B).[41] On the other hand, we also designed a DNA strand (PuAP) (5′-AGAAGAGAAA-GA-3′) that can form the antiparallel duplex but not the parallel one with Py0 under any pH conditions. Note that the nucleobases included in PuP are identical with that in PuAP, which allows us to exclude possible effects of the GC content on the structure and stability of the natural and modified DNA sequences. We introduced LNA (Scheme 1A) modifications at the cytosine bases of Py0, Py1 (5′-TC^{L}TTTCTCTTCT-3′; the LNA-modified bases are shown as C^{L}), Py2 (5′-TC^{L}TTT-C^{L}TCTTCT-3′), Py3 (5′-TC^{L}TTTC^{L}TCTTC^{L}T-3′), and Py4 (5′-TC^{L}TTTC^{L}TC^{L}TTC^{L}T-3′), to investigate the effects of LNA modifications on the structure and stability of the parallel and antiparallel DNA duplexes. Abbreviations and sequences are listed in Table 1.

Structural Analysis. First, the stoichiometry of PuP with fully natural Py0 and LNA-modified Py4 was monitored by UV titration experiments. Figure 1A shows the UV spectra for solutions containing varied ratios of PuP and Py0 with the same total strand concentration constant at 20 μM in Robinson Britton (RB) buffer at pH 5.0 and 4.0 °C. The experiments were conducted at 4.0 °C, instead of 25.0 °C, because some structures of Py0/Pyn (n = 0–4) are not sufficiently stable at 25.0 °C. We found the positive peaks at 254 and 269 nm in the presence of 100% PuP and Py0, respectively. The absorbance at 260 nm with different PuP ratios showed two nearly straight lines intersecting around 50% PuP (Figure 1B), demonstrating formation of a structure with a 1:1 ratio of PuP to Py0. Similar plots with an intersection at 50% were further obtained for PuP/Py0 at pH 7.0 and PuP/Py4 at both pH 5.0 and 7.0 (Figure S1, Supporting Information). These results indicating 1:1 binding are consistent with previous results confirming the formation of a duplex by the use of FRET analysis.[41] On the other hand, an obvious isosbestic point was not observed. This may be because of the metastable structures that can coexist with the most stable structures under these experimental conditions. Because of the coexistence of the metastable structures, the experimental data points should slightly deviate from the two straight lines drawn in Figure 1B. The UV melting curves showed a single transition (Figure 2), whereas a triplex or major metastable structures of the modified DNA strands should exhibit melting curves with two or more transitions.[42] Therefore, these UV melting curves show the formation of bimolecular duplexes under the experimental conditions, the binding ratio of PuP and Pyn (n = 0–4) is 1:1, and the metastable structures are not major species.

The structures of the PuP/Py0 and PuP/Py4 duplexes were evaluated *via* their CD spectra. Figure 3 shows CD spectra of 20 μM PuP/Py0 and PuP/Py4 at pH 5.0 and 7.0 in RB buffer containing 100 mM NaCl at 4.0 °C. The CD spectra of PuP/Py0 and PuP/Py4 exhibited a positive peak around 270 nm with a negative band around 250 nm under all the conditions, indicating formation of a B-form duplex.[43−45] Moreover, CD spectra of PuP/Py0 had a negative peak around 218 nm at pH 5.0, whereas at pH 7.0, this peak was positive. Because it has been shown that a negative peak near 218 nm in a CD

Table 1. Details of the Oligonucleotides Used in This Study

Abbreviation	Sequence[a]	Number of LNA modifications
PuP	5′-AGAAAGAGAAGA-5′	0
Py0	5′-TC TTTC TC TTC T-3′	0
Py1	5′-TC^{L}TTTC TC TTC T-3′	1
Py2	5′-TC^{L}TTTC^{L}TC TTC T-3′	2
Py3	5′-TC^{L}TTTC^{L}TC TTC^{L}T-3′	3
Py4	5′-TC^{L}TTTC^{L}TC^{L}TTC^{L}T-3′	4
PuAP	5′-AGAAGAGAAAGA-5′	0

[a]LNA-modified bases are shown as C^{L}.

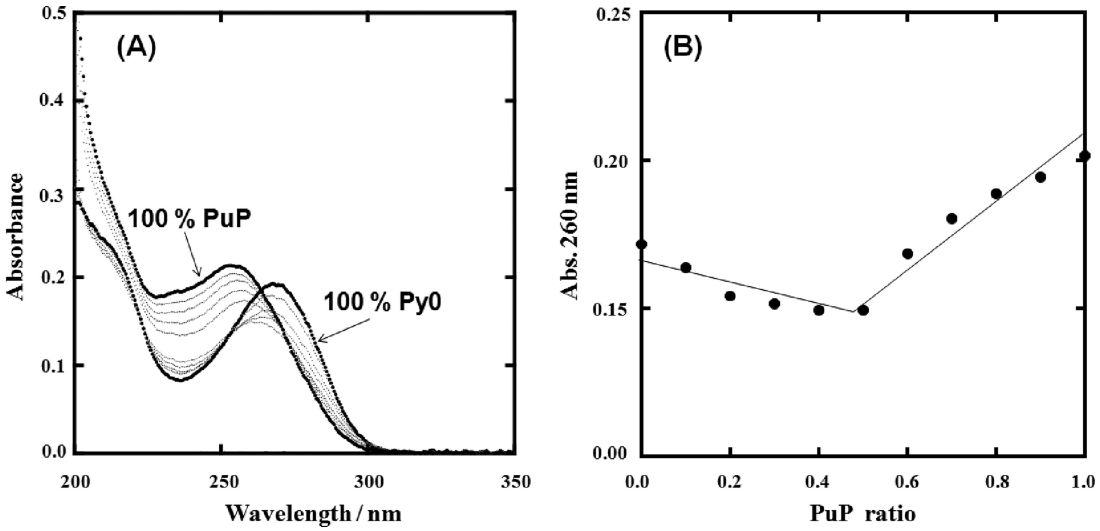

Figure 1. (A) UV Spectra of mixtures containing varied concentration ratios of PuP and Py0 in 40 mM Robinson Britton buffer and 100 mM NaCl at pH 5.0 and 4.0 °C. Total concentration of PuP and Py0 is constant at 20 μM. Bold lines represent the case of 100% PuP and 100% Py0, whereas dotted lines represent all the intermediate ratios. (B) Plot of absorbance values at 260 nm vs PuP ratio.

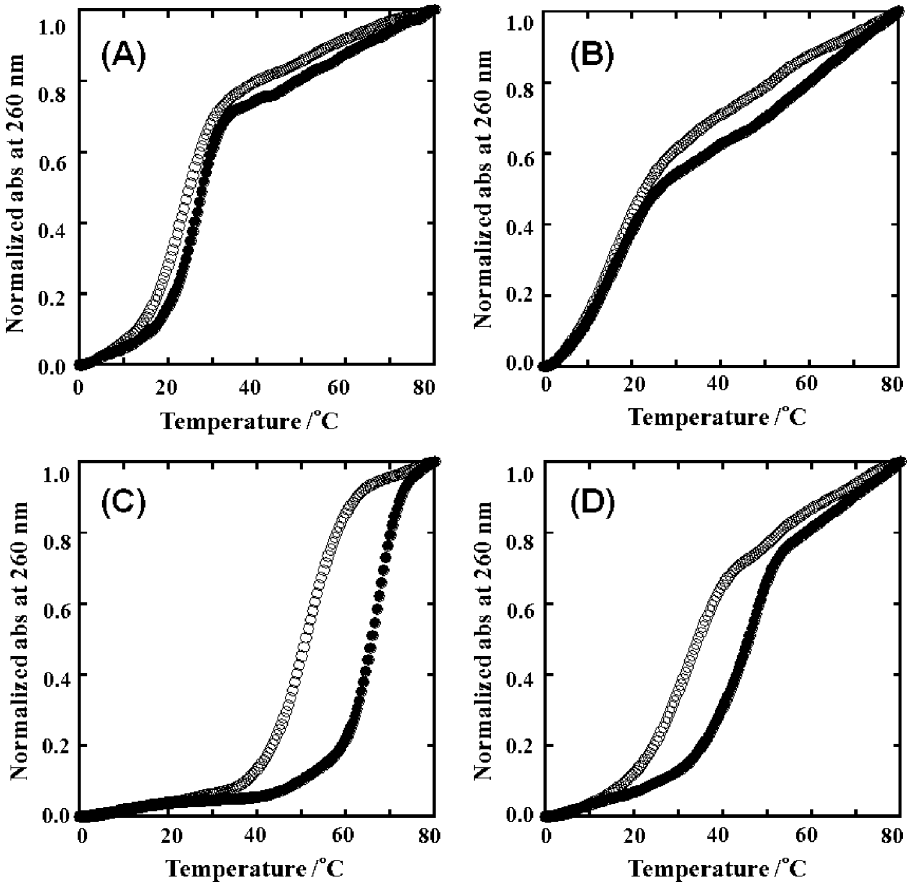

Figure 2. Normalized UV thermal curves of 10 μM PuP/Py0 at pH 5.0 (A) and 7.0 (B) and PuP/Py4 at pH 5.0 (C) and 7.0 (D) in 40 mM Robinson Britton buffer containing 100 mM NaCl. Empty and filled circles represent annealing and melting curves, respectively.

spectrum is a signature of a parallel-stranded duplex through Hoogsteen base pairs,[41,46,47] these results suggest that PuP/Py0 forms a parallel duplex and an antiparallel duplex at pH 5.0 and 7.0, respectively, which are consistent with the previous reports.[41] On the other hand, for PuP/Py4 at both pH 5.0 and 7.0, a negative peak appeared around 218 nm, indicating formation of a parallel duplex at both pH values. In addition, the negative peak near 218 nm of PuP/Py4 was larger than that of PuP/Py0 (Figure 3B). Thus, it is possible to conclude that PuP/Py0 altered the structure from a parallel to an antiparallel duplex by increasing the pH from 5.0 to 7.0, whereas PuP/Py4 maintained its structure of a parallel duplex. These results indicate that the LNA modification specifically stabilizes the parallel duplex. In addition, at pH 5.0, all the CD spectra of

dx.doi.org/10.1021/bi200477g | *Biochemistry* 2011, 50, 7414–7425

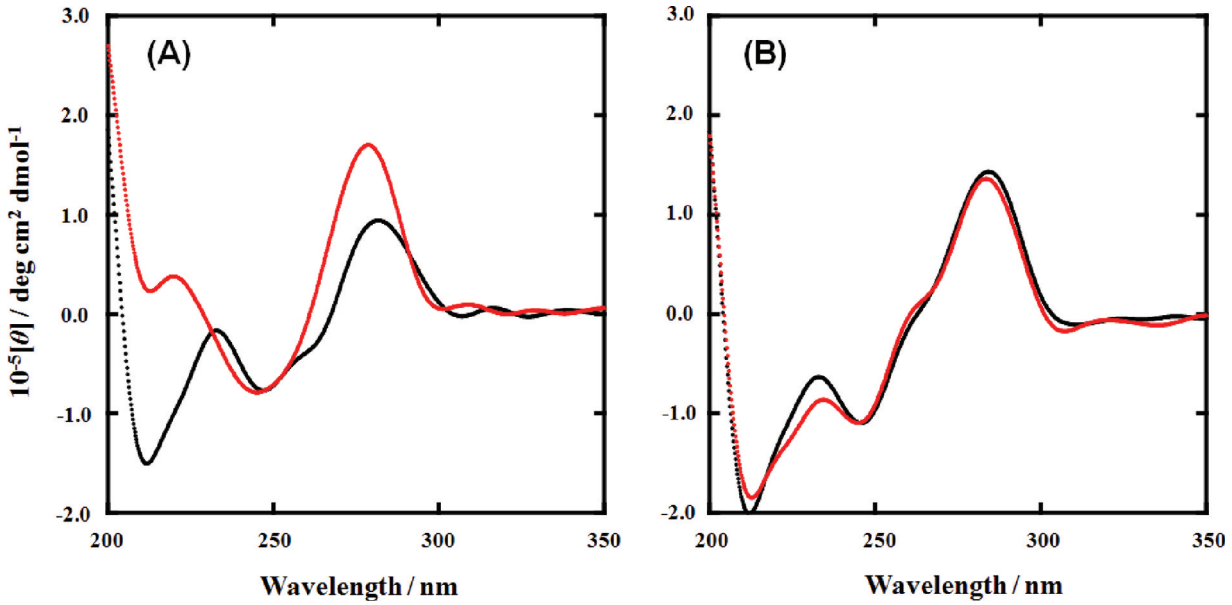

Figure 3. CD spectra of 20 μM PuP/Py0 at pH 5.0 (black line) and 7.0 (red line) (A) and PuP/Py4 at pH 5.0 (black line) and 7.0 (red line) (B) in 40 mM Robinson Britton buffer containing 100 mM NaCl at 4.0 °C.

PuP/Py1, PuP/Py2, and PuP/Py3 had a negative peak at 218 nm, whereas at pH 7.0, the larger negative peak at 218 nm was observed with the larger number of LNA modifications (Figure 4). These results also support the possibility that the LNA modification stabilizes the parallel duplex more than the antiparallel one. Such pH dependency of the duplex formation is due to the protonation of cytosine bases. Thus, these results also suggest the formation of the G-C Hoogsteen base pairs, the stability of which depends on the protonation of cytosine. Although the formation of a parallel dT_{10}/dA_{10} duplex with reverse Watson–Crick base pairs was reported,[48] the parallel mixed sequence duplex used in this study is composed of the Hoogsteen base pairs as shown in the hybridization of the third strand of the parallel triplex.

On the other hand, CD spectra of PuAP/Py0 and PuAP/Py4 did not show a negative peak around 218 nm, in addition to positive and negative peaks around 280 and 250 nm, respectively (Figure S2, Supporting Information). These results for PuAP/Py0 and PuAP/Py4 suggest a formation of the antiparallel duplex under all the conditions tested, further supporting the structural change in PuP/Py0 with the change in pH. From these results, it follows that between pH 5.0 and 7.0, the former is more suitable for systematically comparing the effects of LNA modifications on the thermal stability of the parallel and antiparallel duplexes. This is because at pH 7.0 both parallel and antiparallel duplexes are present whereas at pH 5.0 the dominating structure is the parallel duplex with or without LNA modifications. These CD results show that the sequence designs are successful and these DNA structures are useful for comparing the effects of the LNA modification on the thermodynamics of the canonical and noncanonical DNA structures.

Thermal Analysis. Figure 2 shows UV melting and annealing curves at 260 nm of PuP/Py0 at pH 5.0 (A) and 7.0 (B) and PuP/Py4 at pH 5.0 (C) and 7.0 (D). We observed hysteresis between the melting and annealing curves, and the hysteresis was more significant at pH 5.0 than at pH 7.0. In addition, by comparing the UV melting and annealing curves of PuP/Py0, Py1, Py2, Py3, and Py4, we found that the extent of hysteresis increased with the number of LNA modifications (Figure S3, Supporting Information). Because of the hysteresis, thermodynamic analyses could not be conducted with the melting curves directly. Thus, the apparent half-temperature for melting ($T_{1/2-\mathrm{melt}}$) and the apparent half-temperature for annealing ($T_{1/2-\mathrm{anneal}}$), both of which depend on the temperature gradient, were calculated from the melting and annealing curves, respectively (Table 2). The values of $T_{1/2-\mathrm{melt}}$ for PuP/Py0 and PuP/Py4 at pH 5.0 were evaluated to be 29.0 and 71.5 °C, respectively. Surprisingly, the difference in these values of $T_{1/2-\mathrm{melt}}$ ($\Delta T_{1/2-\mathrm{melt}}$) was 42.5 °C, corresponding to 10.6 °C per LNA modification. To the best of our knowledge, this is the largest stabilization effect of chemical modification on the thermal stability of DNA structures.[3,15,49] On the other hand, UV melting and annealing curves of PuAP/Py0 and PuAP/Py4 at pH 5.0 and 7.0 did not show hysteresis, where all of the differences between the $T_{1/2-\mathrm{melt}}$ and $T_{1/2-\mathrm{anneal}}$ values of PuAP/Py0 and PuAP/Py4 were within 1.5 °C (Figure 5). By comparison of PuAP/Py0 and PuAP/Py4, the values of $\Delta T_{1/2-\mathrm{melt}}$ per LNA modification at pH 5.0 and 7.0 were 4.3 and 3.2 °C, respectively. These results showed that the LNA modification stabilizes modestly the antiparallel duplexes, results comparable with those of previous reports.[3,10,49,50] Note that the degree of the stabilization observed in the parallel duplex is much more significant than that in the antiparallel one, confirming that the effect of LNA modification on the thermal stability of DNA structure depends on the structure of DNA.

Kinetic Analysis of Formation of the Parallel Duplex at pH 5.0. To obtain further insights into the stabilization mechanism of the LNA-modified parallel duplex, we attempted kinetic analyses of the folding and unfolding of the DNA structures by use of the nonequilibrium UV melting and annealing curves. The kinetic analyses of the melting and annealing curves allow us to determine the association rate constant (k_{on}) and dissociation (k_{off}) rate constant, and also the activation energy (E_a) using a two-state (all-or-none) model.[51−54] It is possible to observe a simple one-way reaction

dx.doi.org/10.1021/bi200477g | Biochemistry 2011, 50, 7414–7425

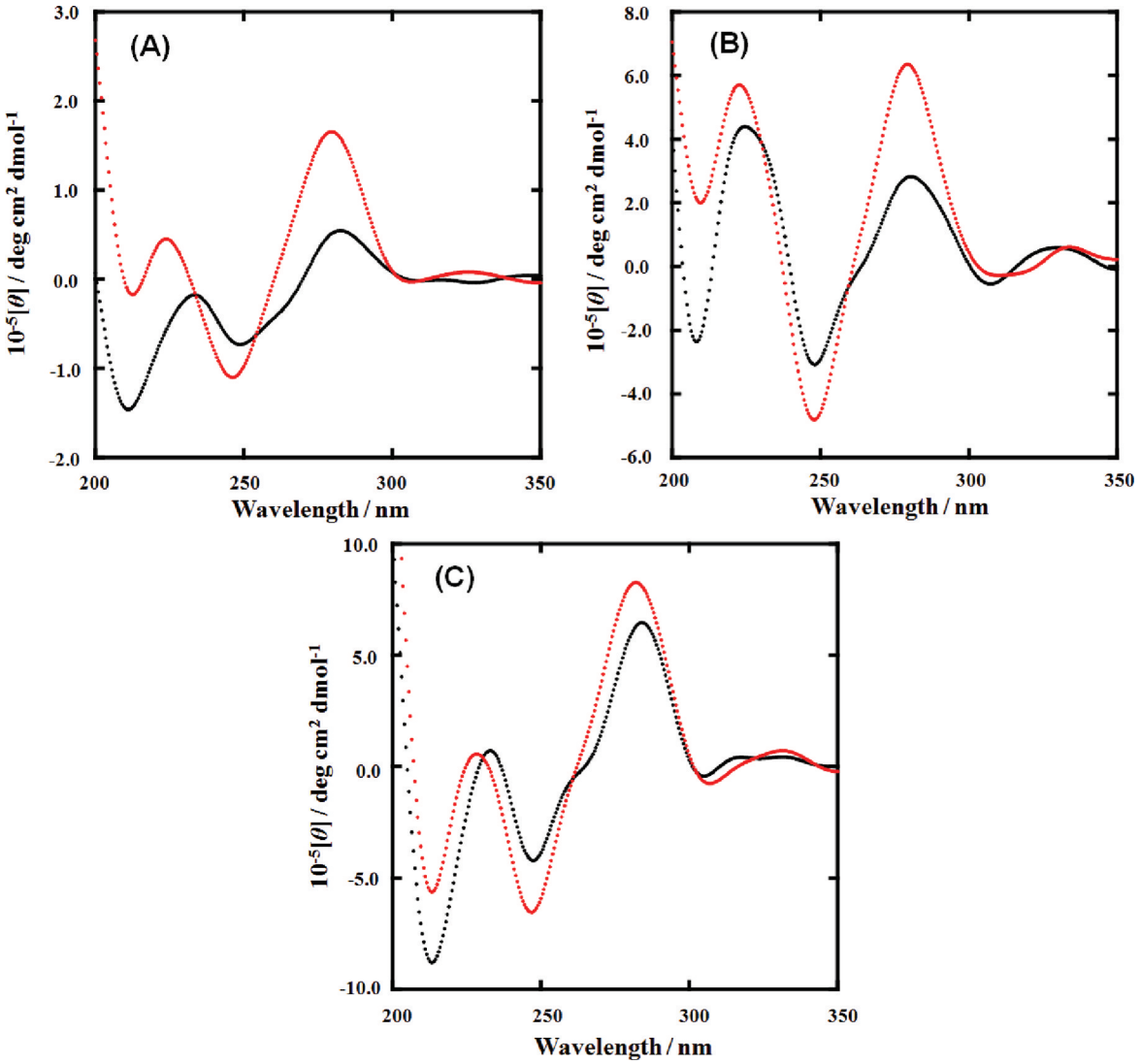

Figure 4. CD spectra of 20 μM PuP/Py1 at pH 5.0 (black line) and 7.0 (red line) (A), PuP/Py2 at pH 5.0 (black line) and 7.0 (red line) (B), and PuP/Py3 at pH 5.0 (black line) and 7.0 (red line) (C) in 40 mM Robinson Britton buffer containing 100 mM NaCl at 4.0 °C.

Table 2. $T_{1/2-melt}$ and $T_{1/2-anneal}$ of the 10 μM PuP/Py*n* (n = 0−4) Mixtures in the Presence of 40 mM Robinson Britton Buffer and 100 mM NaCl at pH 5.0 and 7.0

	pH 5.0		pH 7.0	
abbreviation	$T_{1/2-melt}$ (°C)	$T_{1/2-anneal}$ (°C)	$T_{1/2-melt}$ (°C)	$T_{1/2-anneal}$ (°C)
PuP/Py0	29.0	25.0	18.5	15.9
PuP/Py1	38.0	31.0	14.5	11.5
PuP/Py2	52.5	37.5	26.0	20.0
PuP/Py3	56.5	44.5	30.5	24.4
PuP/Py4	71.5	53.0	48.5	33.4

from a folded state (duplex) to an unfolded state (random coil) with a melting curve, whereas that from a random coil to a duplex can be traced with an annealing curve. This kinetic analysis was reported by Rougée et al.[39] for the first time and has been utilized for kinetic analysis not only for duplex but also for other noncanonical structures.[40,55,56] Generally, the kinetic parameters, association rate constant (k_{on}) and dissociation rate constant (k_{off}) at $T_{1/2-anneal}$ and $T_{1/2-melt}$, respectively, have been evaluated in the previous studies because the rate constant can be estimated accurately around $T_{1/2}$ because of a larger change in absorbance resulting in an accurate analysis. Moreover, the estimations of k_{on} and k_{off} at different temperatures were sufficient to analyze folding and unfolding mechanisms of the structures mentioned above. However, in our study, we compare systematically the kinetic parameters with or without LNA modification (i.e., for PuP/Py0 and PuP/Py4), which results in the large difference in the values of $T_{1/2}$ as shown in Table 2. Therefore, we evaluated k_{on} and k_{off} at 25.0 °C from the extrapolation of the Arrhenius plot derived from k_{on} and k_{off} at each temperature.

Figure 6A shows the plot of $\ln(k_{on}C)$ and $\ln(k_{off})$ versus $1/T$ for PuP/Py0 at pH 5.0 in the 23.5−30.0 °C temperature range. The plot showed a positive slope for $k_{on}C$ and a negative slope for k_{off} indicating negative and positive E_a values, respectively. The k_{on} at $T_{1/2-anneal}$ (25.0 °C) and the k_{off} at $T_{1/2-melt}$ (29.0 °C) were 4.97×10^7 M^{-1} s^{-1} and 21.5 s^{-1}, respectively (Table 3). This implies that the velocity of the product of folding and concentration, $k_{on}C$ (49.7 s^{-1}), is faster than k_{off}, which is the reason behind the hysteresis in the thermal profiles. Moreover, k_{on} and k_{off} at 25.0 °C were 5.00×10^6 M^{-1} s^{-1} and

dx.doi.org/10.1021/bi200477g | *Biochemistry* 2011, 50, 7414–7425

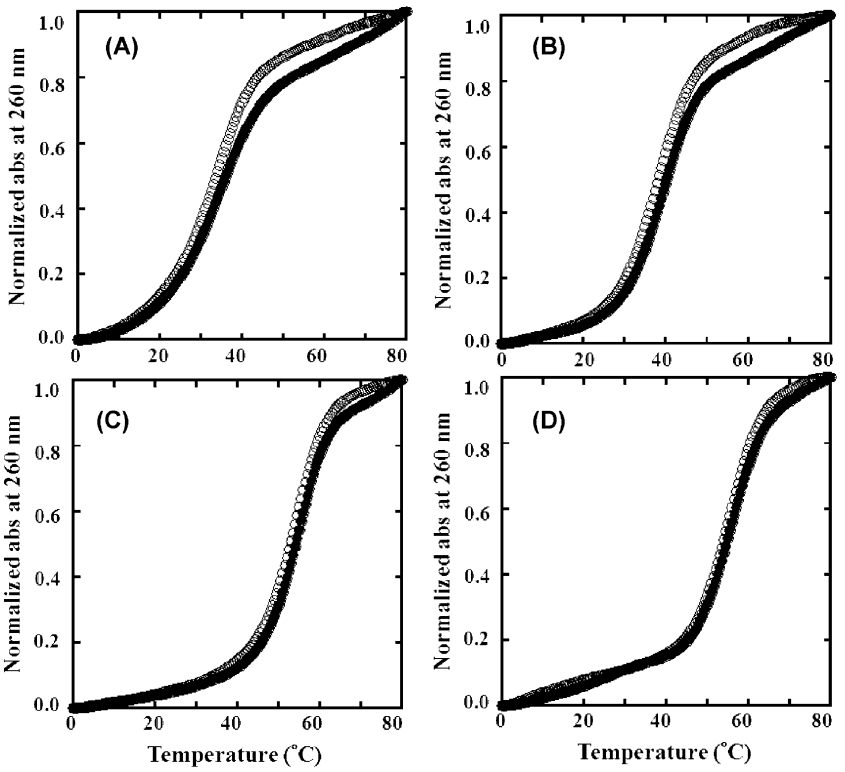

Figure 5. Normalized UV thermal curves of 10 μM PuAP/Py0 at pH 5.0 (A) and 7.0 (B) and PuAP/Py4 at pH 5.0 (C) and 7.0 (D) in 40 mM Robinson Britton buffer containing 100 mM NaCl. Empty and filled circles represent annealing and melting curves, respectively.

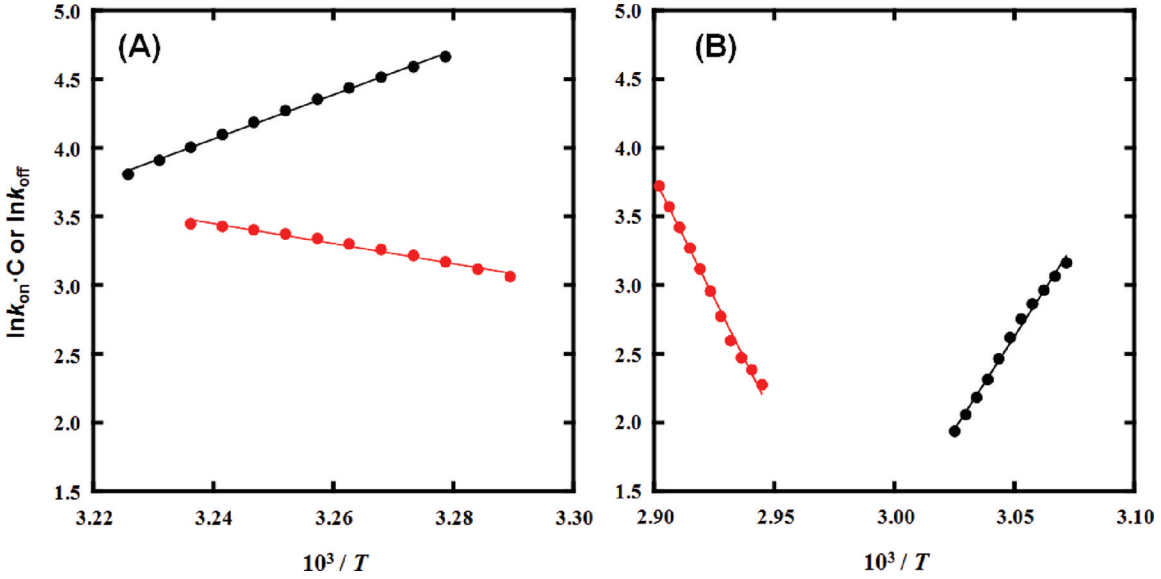

Figure 6. Variation of $k_{on}C$ (black) and k_{off} (red) for PuP/Py0 (A) and PuP/Py4 (B) at pH 5.0 as a function of $1/T$.

11.5 s^{-1}, respectively. These values are similar to previous observations reporting that the k_{on} value for DNA duplex formation is typically around 10^5–10^7 M^{-1} s^{-1} and that the k_{off} value largely depends on the particular DNA sequence.[57,58] These comparisons indicate that the kinetic analysis utilizing the melting and annealing curves with hysteresis is reasonable. Figure 6B shows the plot for PuP/Py4 at pH 5.0 in the 49.5–55.0 and 66.0–72.0 °C ranges for $k_{on}C$ and k_{off}, respectively. The values of k_{on} at $T_{1/2-anneal}$ and k_{off} at $T_{1/2-melt}$ were 2.14×10^7 M^{-1} s^{-1} and 35.6 s^{-1}, respectively. On the other hand, the k_{on} and k_{off} values at 25.0 °C were 5.50×10^9 M^{-1} s^{-1} and 4.96×10^{-6} s^{-1}, respectively. Surprisingly, k_{on} of PuP/Py4 at 25.0 °C was 3 orders of magnitude larger than that of PuP/Py0. On the other hand, k_{off} of PuP/Py4 at 25.0 °C was 6 orders of magnitude smaller than that of PuP/Py0. These results showed that the large stabilization by the LNA modification has a relationship with the increase in k_{on} and large decrease in k_{off}. Previously, kinetic analyses of the formation of the duplex, triplex, and G-quadruplex with LNA modifications have been conducted.[26,59,60] The kinetic parameters showed that the LNA modifications reduce the dissociation rate constant of the triplex and G-quadruplex.[26,59] In addition, the

dx.doi.org/10.1021/bi200477g | *Biochemistry* 2011, 50, 7414–7425

Table 3. Kinetic and Thermodynamic Data for the Formation of DNA/DNA and DNA/LNA Hybrids at pH 5.0[a]

abbreviation	k_{on} (M^{-1} s^{-1})	k_{off} (s^{-1})	E_{on} (kcal mol^{-1})	E_{off} (kcal mol^{-1})	ΔG°_{25} (kcal mol^{-1})	ΔH° (kcal mol^{-1})	$T\Delta S^{\circ}$ (kcal mol^{-1})
PuP/Py0	4.97×10^{6}[b] (4.97×10^{6})	21.5[c] (11.5)	−33.9 ± 0.1	27.4 ± 0.1	−7.74	−61.3	−53.6
PuP/Py4	2.14×10^{7}[d] (5.50×10^{9})	35.6[e] (4.96×10^{-6})	−54.2 ± 0.1	70.2 ± 0.2	−22.0	−94.4	−72.4
PuAP/Py0					−9.51	−63.4	−53.9
PuAP/Py4					−15.8	−92.0	−76.2

[a]The values of k_{on} and k_{off} are reported at $T_{1/2-anneal}$ and $T_{1/2-melt}$, respectively. The values of k_{on} and k_{off} at 25.0 °C are given in parentheses. [b]The k_{on} value was evaluated at 25.0 °C ($T_{1/2-anneal}$). [c]The k_{off} value was evaluated at 29.0 °C ($T_{1/2-melt}$). [d]The k_{on} value was evaluated at 53.0 °C ($T_{1/2-anneal}$). [e]The k_{off} value was evaluated at 71.5 °C ($T_{1/2-melt}$).

RNA G-quadruplexes were more stable than their DNA counterparts as a result of faster k_{on} and slower k_{off},[56] although the values of k_{on} for the LNA and DNA G-quadruplexes could not be directly compared because these rate constants were expressed in different units (M^{-3} s^{-1} for the LNA G-quadruplex and M^{-1} s^{-1} for the DNA G-quadruplex).[60] Thus, the kinetic parameters obtained here indicate that the mechanism of stabilization of the parallel duplex by the LNA modifications is similar to those of other noncanonical DNA structures.

From the slope of the Arrhenius plots of k_{on} and k_{off}, we further estimated the activation energies for the folding (E_{on}) and unfolding (E_{off}) of the duplex, respectively. At pH 5.0, the values of E_{on} obtained for PuP/Py0 and PuP/Py4 were −33.9 ± 0.1 and −54.2 ± 0.1 kcal mol^{-1}, respectively. These negative values suggest that even with LNA modification, formation of the parallel duplex follows the zip-up model, in which the rate-determining step is the formation of a nucleus consisting of several base pairs.[58,61] In addition, the values of E_{off} obtained for PuP/Py0 (27.4 kcal mol^{-1}) and PuP/Py4 (70.2 kcal mol^{-1}) were positive, which are also consistent with the values for the antiparallel duplex.[58] Moreover, by LNA modification, E_{on} and E_{off} decreased by 20.3 kcal mol^{-1} and increased by 42.8 kcal mol^{-1}, respectively. If E_{on} is negative, it reflects the enthalpy energy before the nucleation for formation of the DNA duplex.[57]

On the basis of the kinetic parameters, we further evaluated thermodynamic parameters for the formation of the parallel duplex. The free energy change at 25 °C (ΔG°) was calculated from the equation $\Delta G^{\circ} = -RT \ln K_a = -RT \ln(k_{on}/k_{off})$, where R, T, and K_a are the gas constant, absolute temperature, and apparent equilibrium constant, respectively. The enthalpy change (ΔH°) and entropy change ($T\Delta S^{\circ}$) could be calculated with the following equations: $\Delta H^{\circ} = E_{on} - E_{off}$, and $\Delta G^{\circ}_{T} = \Delta H^{\circ} - T\Delta S^{\circ}$. At pH 5.0 and 25.0 °C, the values of ΔG°_{25}, ΔH°, and $T\Delta S^{\circ}$ for PuP/Py0 were −7.74, −61.3, and −53.6 kcal mol^{-1}, respectively (Table 3). These values for PuP/Py4 at pH 5.0 were −22.0, −94.4, and −72.4 kcal mol^{-1}, respectively. These results show quantitatively that the four LNA modifications stabilize the parallel duplex by 14.3 kcal mol^{-1}, corresponding to 3.6 kcal mol^{-1} per modification. This large stabilization is due to the decrease in ΔH° (33.1 kcal mol^{-1}) that is more favorable than the decrease in $T\Delta S^{\circ}$ (18.8 kcal mol^{-1}). This is consistent with the decrease in E_{on} values by the LNA modification as discussed above. In addition, the enthalpic stabilization of the parallel duplex by the LNA modification is consistent with the cases of the other structures, as we have discussed above.[5,26,60] Therefore, these results indicate that a more efficient stacking of the bases in the LNA-containing parallel duplex led to the more favorable enthalpic term as proposed in the case of other structures,[5,14,15,18,19] although it is possible that other factors such as hydration affect the enthalpy change of the parallel duplex with LNA modifications.

Thermodynamic Analysis of Formation of the Antiparallel Duplex at pH 5.0. Thermodynamic parameters of formation of the antiparallel duplexes of PuAP/Py0 and PuAP/Py4 were evaluated to obtain further insight into the effects of LNA modifications on the thermodynamics of the different DNA structures. Because the melting and annealing curves did not exhibit hysteresis (Figure 5), indicating the heating and cooling are slow enough to reach equilibrium at each temperature, the thermodynamic parameters were evaluated from the curve fitting procedure with an assumption that the folding and unfolding processes of the antiparallel duplex are in a two-state transition.[40] At pH 5.0, the values of ΔG°_{25}, ΔH°, and $T\Delta S^{\circ}$ for formation of the antiparallel PuAP/Py0 duplex were −9.51, −63.4, and −53.9 kcal mol^{-1}, respectively, at 25.0 °C. These values of PuAP/Py4 at pH 5.0 were −15.8, −92.0, and −76.2 kcal mol^{-1}, respectively (Table 3) These results show quantitatively that the four LNA modifications stabilize the antiparallel duplex by 6.29 kcal mol^{-1}, corresponding to 1.6 kcal mol^{-1} per modification. This stabilization effect of LNA modification is smaller than the half of the stabilization observed in the parallel duplex (3.6 kcal mol^{-1} per modification). These parameters for formation of the parallel and antiparallel duplexes demonstrated quantitatively that the LNA modification specifically stabilized the parallel duplex rather than the antiparallel one. Moreover, as shown in the parallel duplex, this stabilization is due to the decrease in ΔH°, which is more favorable than the decrease in $T\Delta S^{\circ}$. This also indicates that the thermodynamic parameters evaluated from the kinetic analysis are reasonable.

Noteworthy is the fact that at pH 5.0 the unmodified antiparallel PuAP/Py0 duplex (ΔG°_{25} = −9.51 kcal mol^{-1}) is thermodynamically more stable than the unmodified parallel PuP/Py0 duplex (ΔG°_{25} = −7.74 kcal mol^{-1}) even with the contribution from the protonation of C bases. On the other hand, the modified parallel PuP/Py4 duplex (ΔG°_{25} = −22.0 kcal mol^{-1}) is more stable by 6.2 kcal mol^{-1} than the modified antiparallel PuAP/Py4 duplex (ΔG°_{25} = −15.8 kcal mol^{-1}) under the same conditions. Therefore, with the LNA modifications, the formation of the parallel duplex is more favorable than that of the antiparallel duplex. This indicates that the parallel orientation of a DNA strand with LNA modification is more applicable to hybridizing a target DNA strand. Recently, Hrdlicka and co-workers showed that α-DNA strands with 2′-amino-β-L-LNA formed stable duplexes with complementary RNA and DNA in a parallel orientation.[62] These results as well as our results described here are promising for the rational design of functional molecules such as more effective antisense and antigene strands, more sensitive strands for the detection of

Table 4. Kinetic and Thermodynamic Data for the Formation of DNA/DNA and DNA/LNA Hybrids at pH 7.0[a]

abbreviation	k_{on} (M^{-1} s^{-1})	k_{off} (s^{-1})	E_{on} (kcal mol^{-1})	E_{off} (kcal mol^{-1})	ΔG°_{25} (kcal mol^{-1})	ΔH° (kcal mol^{-1})	$T\Delta S^{\circ}$ (kcal mol^{-1})
PuP/Py0	94.4×10^{6}[b] (1.63×10^{6})	12.6[c] (1.61)	−32.9 ± 0.1	6.9 ± 0.1	−8.24	−39.8	−31.6
PuP/Py4	21.4×10^{6}[d] (8.89×10^{6})	16.3[e] (0.20)	−31.4 ± 0.1	35.5 ± 0.1	−10.5	−66.9	−56.4
PuAP/Py0					−10.8	−72.3	−61.5
PuAP/Py4					−16.6	−97.3	−80.7

[a]The values of k_{on} and k_{off} are at $T_{1/2-anneal}$ and $T_{1/2-melt}$, respectively. The values of k_{on} and k_{off} at 25.0 °C are given in parentheses. [b]The k_{on} value was evaluated at 15.9 °C ($T_{1/2-anneal}$). [c]The k_{off} value was evaluated at 18.5 °C ($T_{1/2-melt}$). [d]The k_{on} value was evaluated at 33.4 °C ($T_{1/2-anneal}$). [e]The k_{off} value was evaluated at 48.5 °C ($T_{1/2-melt}$).

target DNA and RNA strands, and molecular switch responding to solution pH toward the drug release system.

Stable Parallel Duplex at pH 7.0. Because it was found that the LNA modifications can stabilize specifically the parallel duplex, we further attempted to demonstrate a possible application of this large stabilization by the modification. It is generally considered that the parallel duplex is unstable at physiological pH because the pK_a of C protonation in a DNA strand is around pH 6.5, similar to that in the parallel triplex and i-motif structures.[63,64] Thus, stabilization of these structures at neutral pH and regulation of their stability are required in a broad spectrum of the nucleic acid chemistry and its applications in vivo and in vitro.

Figure 3 shows CD spectra of 20 μM PuP/Py0 and PuP/Py4 at pH 7.0. The large negative peak around 218 nm, which is the signature of the parallel duplex, was observed for only PuP/Py4 at pH 7.0. This CD spectrum at pH 7.0 for PuP/Py4 is almost the same as its CD spectrum at pH 5.0. These CD spectra showed that PuP/Py0 and PuP/Py4 folded to form the antiparallel and parallel duplexes, respectively. These results suggest that even at pH 7.0 the LNA modifications are able to maintain the parallel duplex structure observed at pH 5.0. Thus, we further investigated the kinetics and thermodynamics of the antiparallel and parallel duplexes at pH 7.0 (Table 4). The values of k_{on} and k_{off} at 25.0 °C for formation of the PuP/Py4 duplex were 8.89×10^{6} M^{-1} s^{-1} and 0.20 s^{-1}, respectively. The k_{on} value significantly decreased from that at pH 5.0 (Table 3), whereas the k_{off} increased. These behaviors led to destabilization of the parallel duplex at pH 7.0. The value of ΔG°_{25} for formation of the parallel PuP/Py4 duplex at pH 7.0 was −10.5 kcal mol^{-1}, which is almost the half of that at pH 5.0 (ΔG°_{25} = −22.0 kcal mol^{-1}). This can be due to the decrease in the number of Hoogsteen hydrogen bonds between C and G. Figure 7 shows the Arrhenius plot for PuP/Py4 at pH 7.0. From this plot, E_{on} and E_{off} were evaluated to be −31.4 and 35.5 kcal mol^{-1}, respectively. The value of E_{on} at pH 7.0 is larger than that at pH 5.0. On the other hand, E_{off} at pH 7.0 is smaller than that at pH 5.0, leading to the larger ΔH° at pH 7.0 (−66.9 kcal mol^{-1}) versus that at pH 5.0 (−94.4 kcal mol^{-1}). This change in ΔH° should be due to the deprotonation of C bases, leading to a reduction in the number of hydrogen bonds involved in the Hoogsteen base pairs between C and G. These results quantitatively demonstrate that the LNA modification can induce the stable parallel duplex under physiological conditions at pH 7.0. The value of $T_{1/2-melt}$ of PuP/Py4 at pH 7.0 was 48.5 °C, higher than the physiological temperature (37.0 °C). Noteworthy is the fact that at pH 7.0 the thermodynamic stability of the modified parallel PuP/Py4 duplex (ΔG°_{25} = −10.5 kcal mol^{-1}) is higher than that of the unmodified antiparallel PuP/Py0 duplex (ΔG°_{25} = −8.24 kcal mol^{-1}).

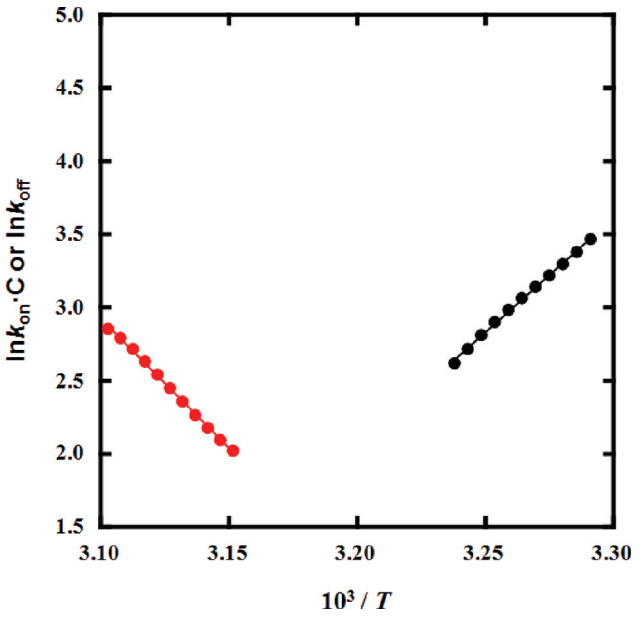

Figure 7. Variation of $k_{on}C$ (black) and k_{off} (red) for PuP/Py4 at pH 7.0 as a function of $1/T$.

The thermodynamic stability of PuP/Py4 at pH 7.0 is, furthermore, comparable with that of the antiparallel PuAP/Py0 duplex (ΔG°_{37} = −10.8 kcal mol^{-1}). Thus, this stable parallel duplex exhibits a new strategy for targeting a DNA sequence by use of a LNA-modified oligonucleotide in a parallel orientation that has comparable thermal stability with an unmodified oligonucleotide hybridizing to a target DNA sequence in an antiparallel manner, although further quantitative studies with various sequences of oligonucleotides and positions of the LNA modification are required.

CONCLUSION

Considering the broad applications and significant success of LNA technology in designing functional molecules based on hybridization with a target sequence, we have attempted to investigate quantitatively and systematically the effects of LNA modifications on the canonical antiparallel and noncanonical parallel DNA duplexes. The hysteresis observed in the melting and annealing curves allowed us to evaluate kinetic parameters for the formation and dissociation of the parallel duplex with LNA modifications. Surprisingly, k_{on} of the LNA-modified parallel duplex at 25.0 °C was 3 orders of magnitude larger than that of the unmodified parallel duplex, whereas k_{off} of the modified parallel duplex at 25.0 °C was 6 orders of magnitude smaller than that of the unmodified one. These results demonstrate a correlation between the strong stabilization by the LNA

modification and the kinetic parameters, the increase in k_{on} and decrease in k_{off}. Moreover, thermodynamic parameters evaluated from the kinetic parameters showed quantitatively that LNA modification stabilizes the parallel duplex by 3.6 kcal mol^{-1} per modification. This large stabilization was due to the decrease in $\Delta H°$ that is more favorable than the decrease in $T\Delta S°$. Because the parallel and antiparallel duplexes have the same GC content, these quantitative parameters demonstrated that LNA modification specifically stabilized the noncanonical parallel duplex. On the basis of this stabilization, we succeeded in stabilizing the parallel duplex by LNA modification at physiological pH, which is useful in the design of an oligonucleotide hybridizing to a target molecule in parallel manner. Recently, it was reported that molecular crowding, which is one of the critical differences between test tube and living cell conditions, stabilizes and destabilizes the parallel and antiparallel duplexes, respectively.[42] Thus, the parallel duplex should be more stabilized by the combination of cell-mimicking molecular crowding and LNA modification. Although further studies are required, these results indicate that the noncanonical DNA structures stabilized by the cellular conditions and chemical modification are useful in the design of new DNA molecules functioning in living cells.

■ ASSOCIATED CONTENT

Ⓢ Supporting Information

UV spectra of mixtures of PuP and Py0 at pH 7.0, CD spectra of PuAP/Py0 and PuAP/Py4 at pH 5.0 and 7.0, and normalized UV thermal curves of PuP/Py*n* (n = 1, 2, or 3) at pH 5.0 and 7.0. This material is available free of charge via the Internet at http://pubs.acs.org.

■ AUTHOR INFORMATION

Corresponding Author

*D.M.: e-mail, miyoshi@center.konan-u.ac.jp; phone, +81-78-303-1426; fax, +81-78-303-1495. N.S.: e-mail, sugimoto@konan-u.ac.jp. S. Maiti: e-mail, souvik@igib.res.in.

Funding

This work was supported in part by Grants-in-Aid for Scientific Research, the "Core Research" project (2009−2014), and the "Academic Frontier" project (2004−2009) from the Ministry of Education, Culture, Sports, Science and Technology, Japan, the Hirao Taro Foundation of the Konan University Association for Academic Research, and the Long-Range Research Initiative Project of Japan Chemical Industry Association. S. Maiti acknowledges the Japan Society for the Promotion of Science for a Japan Society for the Promotion of Science fellowship.

■ ABBREVIATIONS

LNA, locked nucleic acid; SNP, single-nucleotide polymorphism; HPLC, high-performance liquid chromatography; RB, Robinson Britton; CD, circular dichroism.

■ REFERENCES

(1) Singh, S. K., Nielsen, P., Koshkin, A. A., and Wengel, J. (1998) LNA (locked nucleic acids): Synthesis and high-affinity nucleic acid recognition. *Chem. Commun.*, 455−456.

(2) Obika, S., Nanbu, D., Hari, Y., Morio, J. A. K., Doi, T., and Imanishi, T. (1998) Stability and structural features of the duplexes containing nucleoside analogues with a fixed N-type conformation, 2′-*O*,4′-*C*-methyleneribonucleosides. *Tetrahedron Lett. 39*, 5401−5404.

(3) Kaur, H., Babu, B. R., and Maiti, S. (2007) Perspectives on chemistry and therapeutic applications of locked nucleic acid (LNA). *Chem. Rev. 107*, 4672−4697, (and references cited therein).

(4) Koshkin, A. A., Singh, S. K., Nielsen, P., Rajwanshi, V. K., Kumar, R., Meldgaard, M., Olsen, C. E., and Wengel, J. (1998) LNA (locked nucleic acids): Synthesis of the adenine, cytosine, guanine, 5-methylcytosine, thymine and uracil bicyclonucleoside monomers, oligomerisation, and unprecedented nucleic acid recognition. *Tetrahedron 54*, 3607−3630.

(5) Koshkin, A. A., Nielsen, P., Meldgaard, M., Rajwanshi, V. K., Singh, S. K., and Wengel, J. (1998) LNA (locked nucleic acid): An RNA mimic forming exceedingly stable LNA:LNA duplexes. *J. Am. Chem. Soc. 120*, 13252−132553.

(6) Singh, S. K., and Wengel, J. (1998) Universality of LNA-mediated high-affinity nucleic acid recognition. *Chem. Commun.*, 1247−1248.

(7) Wengel, J. (1999) Synthesis of 3′-*C*- and 4′-*C*-branched oligodeoxynucleotides and the development of locked nucleic acid (LNA). *Acc. Chem. Res. 32*, 301−310.

(8) Wengel, J., Petersen, M., Nielsen, K. E., Jensen, G. A., Hakansson, A. E., Kumar, R., Sørensen, M. D., Rajwanshi, V. K., Bryld, T., and Jacobsen, J. P. (2001) LNA (locked nucleic acid) and the diastereoisomeric α-L-LNA: Conformational tuning and high-affinity recognition of DNA/RNA targets. *Nucleosides, Nucleotides Nucleic Acids 20*, 389−396.

(9) Wahlestedt, C., Salmi, P., Good, L., Kela, J., Johnsson, T., Hökfelt, T., Broberger, C., Porreca, F., Lai, J., Ren, K., Ossipov, M., Koshkin, A., Jakobsen, N., Skouv, J., Oerum, H., Jacobsen, M. H., and Wengel, J. (2000) Potent and nontoxic antisense oligonucleotides containing locked nucleic acids. *Proc. Natl. Acad. Sci. U.S.A. 97*, 5633−5638.

(10) Vester, B., and Wengel, J. (2004) LNA (locked nucleic acid): High-affinity targeting of complementary RNA and DNA. *Biochemistry 43*, 13233−13241.

(11) Nielsen, K. E., Rasmussen, J., Kumar, R., Wengel, J., Jacobsen, J. P., and Petersen, M. (2004) NMR studies of fully modified locked nucleic acid (LNA) hybrids: Solution structure of an LNA:RNA hybrid and characterization of an LNA:DNA hybrid. *Bioconjugate Chem. 15*, 449−457.

(12) Petersen, M., Bondensgaard, K., Wengel, J., and Jacobsen, J. P. (2002) Locked nucleic acid (LNA) recognition of RNA: NMR solution structures of LNA:RNA hybrids. *J. Am. Chem. Soc. 124*, 5974−5982.

(13) Braasch, D. A., and Corey, D. R. (2001) Locked nucleic acid (LNA): Fine-tuning the recognition of DNA and RNA. *Chem. Biol. 8*, 1−7.

(14) Kaur, H., Arora, A., Wengel, J., and Maiti, S. (2006) Thermodynamic, counterion, and hydration effects for the incorporation of locked nucleic acid nucleotides into DNA duplexes. *Biochemistry 45*, 7347−7355.

(15) Kaur, H., Wengel, J., and Maiti, S. (2008) Thermodynamics of DNA-RNA heteroduplex formation: Effects of locked nucleic acid nucleotides incorporated into the DNA strand. *Biochemistry 47*, 1218−1227.

(16) Christensen, U., Jacobsen, N., Rajwanshi, V. K., Wengel, J., and Koch, T. (2001) Stopped-flow kinetics of locked nucleic acid (LNA)−oligonucleotide duplex formation: Studies of LNA−DNA and DNA−DNA interactions. *Biochem. J. 354*, 481−484.

(17) Kierzek, E., Ciesielska, A., Pasternak, K., Mathews, D. H., Turner, D. H., and Kierzek., R. (2005) The influence of locked nucleic acid residues on the thermodynamic properties of 2′-O-methyl RNA/RNA heteroduplexes. *Nucleic Acids Res. 33*, 5082−5093.

(18) Kierzek, E., Pasternak, A., Pasternak, K., Gdaniec, Z., Yildirim, I., Turner, D. H., and Kierzek., R. (2009) Contributions of stacking, preorganization, and hydrogen bonding to the thermodynamic stability of duplexes between RNA and 2′-*O*-methyl RNA with locked nucleic acids. *Biochemistry 48*, 4377−4387.

(19) McTigue, P. M., Peterson, R. J., and Kahn, J. D. (2004) Sequence-dependent thermodynamic parameters for locked nucleic acid (LNA)-DNA duplex formation. *Biochemistry 43*, 5388−5405.

(20) Bruylants, G., Boccongelli, M., Snoussi, K., and Bartik, K. (2009) Comparison of the thermodynamics and base-pair dynamics of a full LNA:DNA duplex and of the isosequential DNA:DNA duplex. *Biochemistry 48*, 8473−8482.

(21) Duca, M., Vekhoff, P., Oussedik, K., Halby, L., and Arimondo, P. B. (2008) The triple helix: 50 years later, the outcome. *Nucleic Acids Res. 36*, 5123−5138.

(22) Neidle, S., and Read, M. A. (2000) G-quadruplexes as therapeutic targets. *Biopolymers 56*, 195−208.

(23) Phan, A. T., Kuryavyi, V., and Patel, D. J. (2006) DNA architecture: From G to Z. *Curr. Opin. Struct. Biol. 16*, 288−298.

(24) Qin, Y., and Hurley, L. H. (2008) Structures, folding patterns, and functions of intramolecular DNA G-quadruplexes found in eukaryotic promoter regions. *Biochimie 90*, 1149−1171.

(25) Simonsson, T. (2001) G-quadruplex DNA structures: Variations on a theme. *Biol. Chem. 382*, 621−628.

(26) Torigoe, H., Hari, Y., Sekiguchi, M., Obika, S., and Imanishi, T. (2001) 2′-*O*,4′-*C*-Methylene bridged nucleic acid modification promotes pyrimidine motif triplex DNA formation at physiological pH. *J. Biol. Chem. 276*, 2354−2360.

(27) Obika, S., Uneda, T., Sugimoto, T., Nanbu, D., Minami, T., Doi, T., and Imanishi, T. (2001) 2′-*O*,4′-*C*-Methylene bridged nucleic acid (2′,4′-BNA): Synthesis and triplex-forming properties. *Bioorg. Med. Chem. 9*, 1001−1011.

(28) Sun, B.-W., Babu, B. R., Sørensen, M. D., Zakrzewska, K., Wengel, J., and Sun, J.-S. (2004) Sequence and pH effects of LNA-containing triple helix-forming oligonucleotides:physical chemistry, biochemistry, and modeling studies. *Biochemistry 43*, 4160−4169.

(29) Kumar, N., Nielsen, K. E., Maiti, S., and Petersen, M. (2006) Triplex formation with α-L-LNA (α-L-ribo-configured locked nucleic acid). *J. Am. Chem. Soc. 128*, 14−15.

(30) Alam, M. R., Majumdar, A., Thazhathveetil, A. K., Liu, S.-T., Liu, J.-L., Puri, N., Cuenoud, B., Sasaki, S., Miller, P. S., and Seidman, M. M. (2007) Extensive sugar modification improves triple helix forming oligonucleotide activity in vitro but reduces activity in vivo. *Biochemistry 46*, 10222−10233.

(31) Randazzo, A., Esposito, V., Ohlenschläger, O., Ramachandran, R., and Mayol, L. (2004) NMR solution structure of a parallel LNA quadruplex. *Nucleic Acids Res. 32*, 3083−3092.

(32) Nielsen, J. T., Arar, K., and Petersen, M. (2006) NMR solution structures of LNA (locked nucleic acid) modified quadruplexes. *Nucleic Acids Res. 34*, 2006−2014.

(33) Olejniczak, M., Galka, P., and Krzyzosiak, W. J. (2010) Sequence-non-specific effects of RNA interference triggers and microRNA regulators. *Nucleic Acids Res. 38*, 1−16.

(34) Kumar, N., and Maiti, S. (2007) Role of locked nucleic acid modified complementary strand on quadruplex/Watson Crick duplex equilibrium. *J. Phys. Chem. B 111*, 12328−12337.

(35) Britton, H. T. S., and Robinson, R. A. (1931) Universal buffer solutions and the dissociation constant of veronal. *J. Chem. Soc.*, 1456−1462.

(36) Fernández, C. M., and Martin, V. C. (1977) Preparation d'un tampon universel de force ionique 0,3 M. *Talanta 24*, 747−748.

(37) Nakano, S., Karimata, H., Ohmichi, T., Kawakami, J., and Sugimoto, N. (2004) The effect of molecular crowding with nucleotide length and cosolute structure on DNA duplex stability. *J. Am. Chem. Soc. 126*, 14330−14331.

(38) Miyoshi, D., Karimata, H., and Sugimoto, N. (2006) Hydration regulates thermodynamics of G-quadruplex formation under molecular crowding conditions. *J. Am. Chem. Soc. 128*, 7957−7963.

(39) Rouge, M., Faucon, B., Mergny, J. L., Barcelo, F., Giovannangeli, C., Garestier, T., and Hèlène, C. (1992) Kinetics and thermodynamics of triple-helix formation: Effects of ionic strength and mismatches. *Biochemistry 31*, 9269−9278.

(40) Mergny, J.-L., and Lacroix, L. (2003) Analysis of thermal melting curves. *Oligonucleotides 13*, 515−537.

(41) Ohmichi, T., Kawamoto, Y., Peng, W., Miyoshi, D., Karimata, H., and Sugimoto, N. (2005) DNA-based biosensor for monitoring pH *in vitro* and in living cells. *Biochemistry 44*, 7125−7130.

(42) Miyoshi, D., Nakamura, K., Karimata, H. T., Ohmichi, T., and Sugimoto, N. (2009) Hydration of Watson-Crick base pairs and dehydration of Hoogsteen base pairs inducing structural polymorphism under molecular crowding conditions. *J. Am. Chem. Soc. 131*, 3522−3531.

(43) Saenger, W. (1984) in *Principles of Nucleic Acid Structure*, Springer-Verlag, New York.

(44) Bloomfield, V. A., Crothers, D. M., and Tinoco, I., Jr. (2000) in *Nucleic Acids: Structures, Properties, and Functions*, University Science Books, Sausalito, CA.

(45) Nakano, S., Kanzaki, T., and Sugimoto, N. (2004) Influences of ribonucleotide on a duplex conformation and its thermal stability: Study with the chimeric RNA-DNA strands. *J. Am. Chem. Soc. 126*, 1088−1095.

(46) Li, W., Miyoshi, D., Nakano, S., and Sugimoto, N. (2003) Structural competition involving G-quadruplex DNA and its complement. *Biochemistry 42*, 11736−11744.

(47) Okumoto, Y., Tanabe, Y., and Sugimoto, N. (2003) Factors that contribute to efficient catalytic activity of a small Ca^{2+}-dependent deoxyribozyme in relation to its RNA cleavage function. *Biochemistry 42*, 2158−2165.

(48) Van de Sande, J. H., Ramsing, N. B., Germann, M. W., Elhorst, W., Kalisch, B. W., Kitzing, E. V., Pon, R. T., Clegg, R. C., and Jovin, T. M. (1988) Parallel stranded DNA. *Science 241*, 551−557.

(49) Kumar, N., Petersen, M., and Maiti, S. (2009) Tunable c-*MYC* LNA *i*-motif. *Chem. Commun.*, 1532−1534.

(50) Petersen, M., and Wengel, J. (2003) LNA: A versatile tool for therapeutics and genomics. *Trends Biotechnol. 21*, 74−81.

(51) Cantor, C. R., and Schimmel, P. R. (1980) in *Biophysical Chemistry*, Part III, W. H. Freeman and Co., San Francisco.

(52) Pörschke, D., and Eigen, M. (1971) Co-operative non-enzymic base recognition III. Kinetics of the helix-coil transition of the oligoribouridylic·oligoriboadenylic acid system and of the oligoriboadenylic acid alone at acidic pH. *J. Mol. Biol. 62*, 361−381.

(53) Craig, M. E., Crothers, D. M., and Doty, P. (1971) Relaxation kinetics of dimer formation by self complementary oligonucleotides. *J. Mol. Biol. 62*, 383−401.

(54) Anshelevich, V. V., Vologodskii, A. V., Lukashin, A. V., and Frank-Kamenetskii, M. D. (1984) Slow relaxational processes in the melting of linear biopolymers: A theory and its application to nucleic acids. *Biopolymers 23*, 39−58.

(55) Phan, A. T., and Mergny, J.-L. (2002) Human telomeric DNA: G-quadruplex, i-motif and Watson-Crick double helix. *Nucleic Acids Res. 30*, 4618−4625.

(56) Mergny, J.-L., and Lacroix, L. (1998) Kinetics and thermodynamics of i-DNA formation: Phosphodiester versus modified oligodeoxynucleotides. *Nucleic Acids Res. 26*, 4797−4803.

(57) Turner, D. H. (2000) in *Nucleic Acids: Structure, Properties and Functions* (Bloomfield, V. A., Crothers, D. M., and Tinoco, I., Eds.) University Science Book, Sausalito, CA.

(58) Gu, X.-B., Nakano, S., and Sugimoto, N. (2007) Consecutive GC base pairs determine the energy barrier of DNA duplex formation under molecularly crowded conditions. *Chem. Commun.*, 2750−2752.

(59) Brunet, E., Alberti, P., Perrouault, L., Babu, R., Wengel, J., and Giovannangeli, C. (2005) Exploring cellular activity of locked nucleic acid-modified triplex-forming oligonucleotides and defining its molecular basis. *J. Biol. Chem. 280*, 20076−20085.

(60) Petraccone, L., Erra, E., Randazzo, A., and Giancola, C. (2006) Energetic aspects of locked nucleic acids quadruplex association and dissociation. *Biopolymers 83*, 584−594.

(61) Williams, A. P., Longfellow, C. E., Freier, S. M., Kierzek, R., and Turner, D. H. (1989) Laser temperature-jump, spectroscopic, and thermodynamic study of salt effects on duplex formation by dGCATGC. *Biochemistry 28*, 4283−4291.

(62) Kumar, T. S., Østergaard, M. E., Sharma, P. K., Nielsen, P., Wengel, J., and Hrdlicka, P. J. (2009) Parallel RNA-strand recognition by 2′-amino-*β*-L-LNA. *Bioorg. Med. Chem. Lett. 19*, 2396−2399.

(63) Sugimoto, N., Wu, P., Hara, H., and Kawamoto, Y. (2001) pH and cation effects on the properties of 64 parallel pyrimidine motif DNA triplexes. *Biochemistry 40*, 9396−9405.

(64) Rajendran, A., Nakano, S., and Sugimoto, N. (2010) Molecular crowding of the cosolutes induces an intramolecular i-motif structure of triplet repeat DNA oligomers at neutral pH. *Chem. Commun. 46*, 1299−1301.